0013-7227/06/$15.00/0
Printed in U.S.A.

Endocrinology 147(5):2583–2590

doi: 10.1210/en.2005-1627

Parathyroid Hormone Increases β-Catenin Levels through Smad3 in Mouse Osteoblastic Cells

Takako Tobimatsu, Hiroshi Kaji, Hideaki Sowa, Junko Naito, Lucie Canaff, Geoffrey N. Hendy, Toshitsugu Sugimoto, and Kazuo Chihara

Division of Endocrinology/Metabolism, Neurology, and Hematology/Oncology, Department of Clinical Molecular Medicine, Kobe University Graduate School of Medicine (T.T., H.K., H.S., J.N., K.C.), Kobe 650-0017, Japan; Departments of Medicine, Physiology, and Human Genetics, McGill University, and Calcium Research Laboratory and Hormones and Cancer Research Unit, Royal Victoria Hospital (L.C., G.N.H.), Montréal, Québec, Canada H3A 1A1; and Department of Endocrinology, Metabolism, and Hematological Oncology, Shimane University School of Medicine (T.S.), Shimane 693-8501, Japan

PTH, via the PTH/PTH-related protein receptor type 1 that couples to both protein kinase A (PKA) and protein kinase C (PKC) pathways, and the canonical Wnt-β-catenin signaling pathway play important roles in bone formation. In the present study we have examined the interaction between the PTH and Wnt signaling pathways in mouse osteoblastic MC3T3-E1 cells. PTH dose- and time-dependently increased the concentrations of β-catenin. The PKA activator, forskolin, and the PKC activator, phorbol 12-myristate-13-acetate, as well as the PTH analog, [Nle^{8,18},Tyr^{34}]human PTH-(3–34)amide, all increased β-catenin levels. Both H-89, a specific PKA inhibitor, and PKC inhibitors, staurosporine and calphostin C, antagonized PTH stimulation of β-catenin levels. TGF-β as well as transfection of the TGF-β-signaling molecule, Smad3, enhanced β-catenin levels, and this was antagonized by transfection of a dominant-negative Smad3. The transcriptional activity of transfected dominant-active β-catenin was enhanced by PTH, an effect that was antagonized by cotransfection of a dominant-negative Smad3. PTH as well as $LiCl_2$, which mimics the effects of the Wnt-β-catenin pathway, rescued the dexamethasone- and etoposide-induced apoptosis of osteoblastic cells. In conclusion, the data demonstrate that PTH stimulates osteoblast β-catenin levels via Smad3, and that both PKA and PKC pathways are involved. The canonical Wnt-β-catenin pathway is likely to be involved in the anti-apoptotic actions of PTH by acting through Smad3 in osteoblasts. (*Endocrinology* 147: 2583–2590, 2006)

IT IS WELL ESTABLISHED that daily injections of low-dose PTH increase bone mass in animals and humans (1). The anabolic action of PTH is exerted partly through local growth factors and transcriptional regulators as well as an antiapoptotic action in osteoblasts (2). However, the precise mechanisms by which PTH exerts its anabolic action on bone are incompletely understood. Wnts are a family of secreted glycoproteins that act in a paracrine fashion and mediate cellular interactions during development (3). Wnt proteins initiate a canonical (β-catenin regulated) signaling cascade by binding to seven-transmembrane spanning receptors of the Frizzled family together with coreceptors, members of the low-density lipoprotein receptor-related protein (LRP) family, LRP5 and LRP6, which results in the stabilization of cytosolic β-catenin. Interaction of β-catenin with the high-mobility group box transcription factors of the lymphoid enhancer-binding factor (Lef)/T cell factor (Tcf) family allows translocation of the complex into the nucleus to subsequently regulate the transcription of Wnt target genes (4). Inactivating mutations in the Wnt receptor, LRP5, decrease bone mass during growth and cause the autosomal recessive disorder osteoporosis-pseudoglioma syndrome (5). Conversely, activating mutations in LRP5 are linked to autosomal-dominant, high bone mass traits (6). Recent studies of a variety of mouse models have provided evidence that Wnt signaling is important for the determination of skeletal cell fate and for inducing osteoblast, but suppressing chondrocyte, differentiation in osteochondroprogenitors (7, 8). In addition, Wnt signaling may be involved in the coupling of mechanical force to anabolic activity in the skeleton (9). These findings indicate that Wnt-β-catenin signaling pathways are important in bone formation. However, whether PTH regulates the Wnt-β-catenin signal is not clear.

We recently reported that Smad3, a crucial TGF-β-signaling molecule, promotes markers of osteoblast differentiation, for example, the production of type I collagen, alkaline phosphatase activity, and mineralization in mouse osteoblastic MC3T3-E1 cells (10, 11). Moreover, mice with targeted disruption of Smad3 exhibit osteopenia caused by decreased bone formation (12). These findings suggest that the Smad3 molecule is a promoter of bone formation.

In the present study we have examined the effects of PTH on β-catenin and the role that Smad3 plays on the effects of PTH in mouse osteoblastic MC3T3-E1 cells.

First Published Online February 16, 2006

Abbreviations: ALK-5, TGF-β type I receptor kinase; db-cAMP, N^6,$O^{2'}$-dibutyryl cAMP; FBS, fetal bovine serum; GAPDH, glyceraldehyde-3-phosphate dehydrogenase; h, human; Lef-1, lymphoid enhancer-binding factor 1; LRP, low-density lipoprotein receptor-related protein; MH2, MAD homology 2; PKA, protein kinase A; PKC, protein kinase C; PMA, phorbol 12-myristate-13-acetate; Sp diastereoisomer of adenosine cyclic 3′,5′-phosphorothioate; Tcf, T cell factor; TUNEL, transferase-mediated deoxyuridine triphosphate nick end labeling.

***Endocrinology* is published monthly by The Endocrine Society (http://www.endo-society.org), the foremost professional society serving the endocrine community.**

Materials and Methods

Materials

MC3T3-E1 cells were provided by Dr. H. Kodama (Ohu Dental College, Koriyama, Japan). Human (h) PTH-(1–34), [$Nle^{8,18}Tyr^{34}$]hPTH-(3–34)amide [PTH-(3–34)], phorbol 12-myristate 13-acetate (PMA), forskolin, N^6,$O^{2'}$-dibutyryl cAMP (db-cAMP), staurosporine, H89, cycloheximide, antiphosphorylated β-catenin and anti-β-actin antibodies were obtained from Sigma-Aldrich Corp. (St. Louis, MO), and the Sp diastereoisomer of adenosine cyclic 3′,5′-phosphorothioate (Sp-cAMPS) was obtained from Biolog Life Science Institute (Bremen, Germany). Calphostin C and SB431542 were purchased from Calbiochem-Novabiochem Corp. (San Diego, CA) and Tocris Cookson Ltd. (Bristol, UK), respectively. Anti-β-catenin and anti-phosphorylated Smad3 antibodies were obtained from Santa Cruz Biotechnology, Inc. (Santa Cruz, CA). Anti-Smad3 and anti-TCF antibodies were purchased from Zymed Laboratories (San Francisco, CA) and Exalpha Biologicals, Inc. (Watertown, MA), respectively. All other chemicals used were of analytical grade.

Cell culture

Mouse osteoblastic MC3T3-E1 cells were cultured in α-MEM (containing 50 μg/ml ascorbic acid) with 10% fetal bovine serum (FBS) and 1% penicillin-streptomycin (Invitrogen Life Technologies, Inc., Gaithersburg, MD). The medium was changed twice a week.

Constructs and transient or stable transfection

The vectors expressing Myc-tagged Smad3 and a mutant form of Myc-tagged Smad3 (Smad3ΔC), in which the MAD homology 2 (MH2) domain corresponding to amino acid residues 278–425 had been removed, were described previously (13, 14). Myc-Smad3, Myc-Smad3ΔC, and empty vector (pCDNA3.1$^+$; each 3 μg) were transfected into MC3T3-E1 cells with Lipofectamine (Invitrogen Life Technologies, Inc., Grand Island, NY). Six hours later, the cells were fed fresh α-MEM containing 10% FBS. Forty-eight hours later, the transiently transfected cells were used for experiments. For experiments with stably transfected cells, after incubation in α-MEM containing 10% FBS for 48 h, the cells were passaged, and clones were selected in α-MEM supplemented with G418 (0.3 mg/ml; Invitrogen Life Technologies, Inc.) and 10% FBS. To rule out the possibility of clonal variation, at least three independent clones for each stable transfection were characterized. Empty vector-transfected cells were used as the control.

Protein extraction and Western blot analysis

Cells were lysed with radioimmunoprecipitation buffer containing 0.5 mM phenylmethylsulfonylfluoride, Complete protease inhibitor mixture (Roche Applied Science, Tokyo, Japan), 1% Triton X-100, and 1 mM sodium orthovanadate. Cell lysates were centrifuged at 12,000 × *g* for 20 min at 4 C, and the supernatants were stored at −80 C. Protein quantitation was performed with bicinchoninic acid protein assay reagent (Pierce Chemical Co., Rockford, IL). Twenty-microgram protein aliquots were denatured in sodium dodecyl sulfate sample buffer and separated on 10% polyacrylamide-sodium dodecyl sulfate gels. Proteins were transferred in 25 mM Tris, 192 mM glycine, and 20% methanol to polyvinylidene difluoride. Blots were blocked with 20 mM Tris-HCl (pH 7.5) and 137 mM NaCl plus 0.1% Tween 20 containing 3% dried milk powder. The antigen-antibody complexes were visualized using the appropriate secondary antibodies (Sigma-Aldrich Corp.) and the enhanced chemiluminescence detection system, as recommended by the manufacturer (Amersham Biosciences, Arlington Heights, IL). The results depicted in each figure are representative of at least three separate cell preparations. Each experiment was repeated three times.

RNA extraction and semiquantitative RT-PCR

Total RNA was prepared from cells using the acid guanidinium-thiocyanate-phenol-chloroform extraction method. RT of 5 μg cultured cell total RNA was carried out for 50 min at 42 C and then for 15 min at 70 C using the SuperScript First Strand Synthesis system for RT-PCR (Invitrogen Life Technologies, Inc.), which contained RT buffer, oligo(deoxythymidine)$_{12–18}$, 5× first-strand solution, 10 mM deoxy-NTP, 0.1 M dithiothreitol, SuperScript II (RT enzyme), and ribonuclease H (ribonuclease inhibitor). PCR using primers to unique sequences in each cDNA was carried out in a volume of 10 μl reaction mixture for PCR (supplied by TaKaRa, Otsu, Japan), supplemented with 2.5 U TaKaRa *Taq*, 1.5 mM of each deoxy-NTP (TaKaRa), and PCR buffer [10×; 100 mM Tris-HCl (pH 8.3), 500 mM KCl, and 15 mM $MgCl_2$]; 25 ng of each primer and 1 μl template (from a 50-μl RT reaction) were used. Thermal cycling conditions and primer sequences were as follows: 1) initial denaturation at 96 C for 2 min; 2) cycling for cDNA, specific number of cycles: 96 C for 1 min, cDNA-specific annealing temperature for 2 min, and 72 C for 2 min; and 3) final extension at 72 C for 5 min. Primer sequences, annealing temperature, and cycle numbers were as follows: β-catenin, 5′-GTGCAATTCCTGAGCTGACA-3′ and 5′-CTTAAAGATGGCCAGCAAGC-3′ (58 C; 27 cycles); and glyceraldehyde-3-phosphate dehydrogenase (GAPDH), 5′-ATCCCATCACCATCTTCCAGGAG-3′ and 5′-CCTGCTTCACCACCTTCTTGATG-3′ (47 C; 26 cycles). For semiquantitative RT-PCR, the number of cycles was chosen so that amplification remained well within the linear range, as assessed by densitometry (National Institutes of Health Image J, version 1.08i, public domain program). An equal volume from each PCR was analyzed by 6% nondenaturing PAGE, and ethidium bromide-stained PCR products were evaluated. Marker gene expression was normalized to GAPDH expression in each sample.

Transient transfection and luciferase assay

MC3T3-E1 cells were seeded at a density of 2×10^5/six-well plate. Twenty-four hours later, the cells were transfected with 3 μg of the Tcf-4-responsive luciferase reporter plasmid (pGL3-OT) (15), the activated β-catenin DNA (3 μg) (16), and the pCH110 β-galactosidase-expressing plasmid (1 μg) using Lipofectamine (Invitrogen Life Technologies). Fifteen hours later, the medium was changed to α-MEM containing 4% FBS, and the cells were incubated for an additional 9 h. Thereafter, the cells were cultured for 24 h in the absence or presence of PTH-(1–34) in α-MEM containing 0.2% FBS. The cells were lysed, and luciferase activity was measured and normalized to the relative β-galactosidase activity as previously described (17).

Determination of osteoblast apoptosis

Trypan blue staining [Invitrogen Life Technologies, Inc.; 0.1% (wt/vol) final concentration] was used for quantification of cell viability (14). In brief, a drop of the cell suspension was mixed with a drop of the trypan blue solution at a ratio of 1:1. Total numbers of viable and nonviable cells were counted under light microscopy. In apoptotic cells, DNA is cleaved into histone-associated fragments. A more specific method to detect apoptosis, transferase-mediated deoxyuridine triphosphate nick end labeling (TUNEL) staining was also used. In brief, cells were cultured on round coverglasses (Fisher Scientific, Pittsburgh, PA) in six-well plates, and the coverglasses with cells attached were rinsed twice with ice-cold PBS, followed by fixation with 4% neutral formaldehyde. Then the fixed cell layers on the glasses were stained. The TUNEL reaction was performed using an Apoptosis In Situ Detection kit (Wako Biochemicals, Osaka, Japan) following the standard protocol, as previously described (14). In each experiment, apoptotic cells were counted in randomly selected fields using a hemocytometer and were expressed as percentages compared with total cells. Each experiment was performed at least three times.

Statistics

Data were expressed as the mean ± SEM. Statistical analysis was performed using ANOVA.

Results

Effects of PTH on levels of β-catenin and Lef-1 in mouse osteoblastic cells

First, we examined the effects of PTH on the level of β-catenin protein in MC3T3-E1 cells by Western blot analysis. PTH-(1–34) treatment increased β-catenin levels in a time-dependent fashion from 15 min to 48 h (Fig. 1A) and in

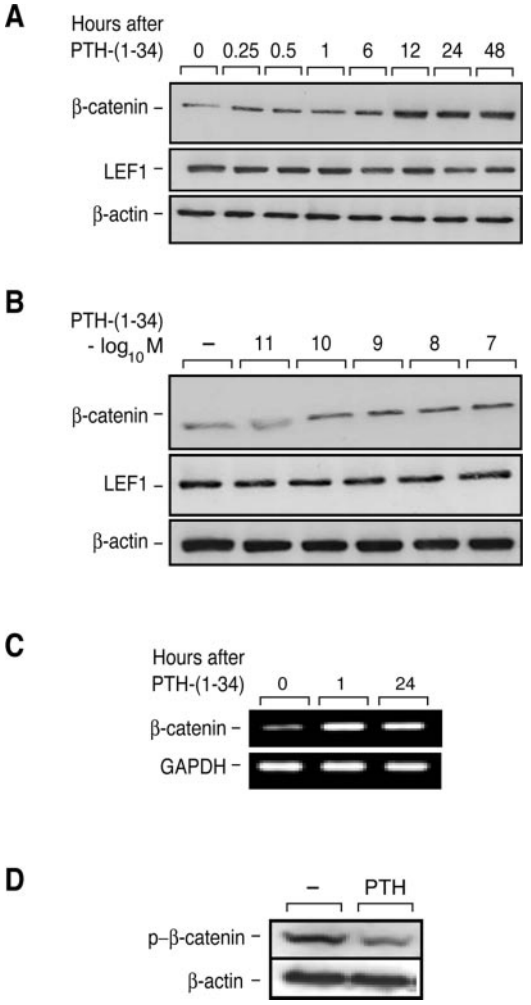

FIG. 1. PTH increases β-catenin expression in a time- and dose-dependent manner in osteoblasts. Confluent MC3T3-E1 cells were cultured in serum-free α-MEM with (A) 10^{-8} M PTH-(1–34) for the indicated times or (B) with PTH-(1–34) at the indicated concentrations for 1 h. Protein extraction of the cells and Western blot analysis were performed as described in *Materials and Methods*. C, Confluent MC3T3-E1 cells were cultured with 10^{-8} M PTH-(1–34) for 1 and 24 h. RNA extraction and semiquantitative RT-PCR analyses were performed as described in *Materials and Methods*. D, Confluent MC3T3-E1 cells were cultured without (−) or with 10^{-8} M PTH-(1–34) for 1 h. Protein extraction of the cells and Western blot analysis were performed as described in *Materials and Methods*.

a concentration-dependent manner from 10^{-10} to 10^{-7} M (Fig. 1B), with a 2.2-fold increase with the 10^{-10}-M dose. However, PTH-(1–34) did not affect Lef-1 protein levels (Fig. 1, A and B) or those of TCF1/4 (data not shown). The level of β-catenin did not change in cells not treated with PTH-(1–34) throughout the 0- to 48-h time course (Fig. 1A and data not shown). PTH induced the levels of β-catenin mRNA assessed by semiquantitative RT-PCR (Fig. 1C). Glycogen synthase kinase-3β destabilizes β-catenin by phosphorylating it at select serine and threonine residues (18). PTH reduced the phosphorylation of β-catenin (serine 45; Fig. 1D). These findings indicated that PTH induces β-catenin through suppression of degradation of the protein as well as by induction of RNA synthesis.

Roles of protein kinase A (PKA) and protein kinase C (PKC) in the induction of β-catenin levels by PTH

The PTH signals are transduced via the PTH/PTH-related protein receptor type 1 through PKA and PKC pathways (1). Therefore, we investigated whether PTH would up-regulate the level of β-catenin through one or both of these pathways. Dibutyryl cAMP and Sp-cAMPS, activators of the PKA pathway, as well as forskolin increased the level of β-catenin in MC3T3-E1 cells (Fig. 2A). Moreover, PMA, an activator of the PKC pathway, increased the level of β-catenin in these cells. PTH-(3–34) stimulated PTH-induced PKC signaling, but not PTH-induced PKA signaling. Therefore, we examined the effects of PTH-(3–34) on the level of β-catenin in MC3T3-E1 cells. The β-catenin level was enhanced by PTH-(3–34) 2.3-fold in these cells (Fig. 2B), providing additional evidence that PTH induction of PKC was involved. Next, we used staurosporine and H89, inhibitors of the PKC and PKA pathways, respectively. H89 as well as staurosporine antagonized the 2-fold increase in β-catenin induced by PTH (Fig. 3A), confirming the involvement of both pathways. Similar results were obtained at 24 h (data not shown). Moreover, calphostin C, a specific PKC inhibitor, antagonized the 2-fold increase in β-catenin induced by PTH (Fig. 3B).

Effects of TGF-β and Smad3 on β-catenin levels in mouse osteoblastic cells

We previously demonstrated that PTH promotes the expression of Smad3 in MC3T3-E1 cells, and that PTH-Smad3 axis exerts antiapoptotic effects in osteoblasts (14). Therefore, we examined the effects of TGF-β, a ligand that induces the activation of Smad3. TGF-β treatment increased β-catenin levels in a dose-dependent (Fig. 4A) and a time-dependent manner (from 6–48 h; Fig. 4B). TGF-β induced the levels of total Smad3 and phosphorylated Smad3 from 1 h (data not shown). The effects of PTH and TGF-β were not additive at

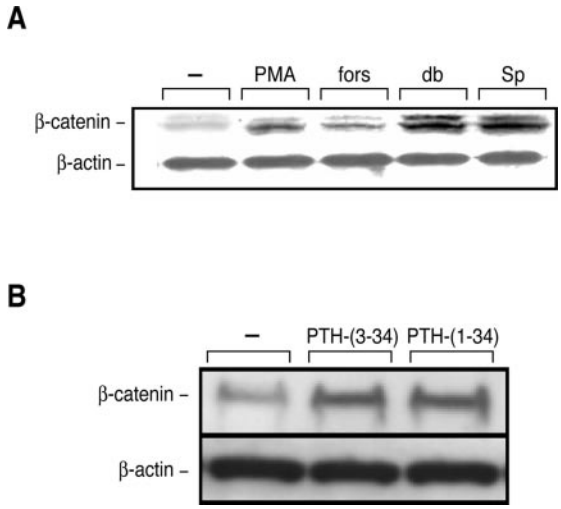

FIG. 2. Effects of PKA and PKC activators as well as PTH-(3–34) on the level of β-catenin in osteoblasts. Confluent MC3T3-E1 cells were cultured in serum-free α-MEM for 12 h, then treated without (−) or with (A) 10^{-6} M PMA, 10^{-5} M forskolin (fors), 10^{-4} M db-cAMP (db), or 10^{-5} M Sp-cAMPS (Sp) or (B) 10^{-7} M PTH-(3–34) or 10^{-8} M PTH-(1–34) for 1 h. Protein extraction of the cells and Western blot analysis were performed as described in *Materials and Methods*.

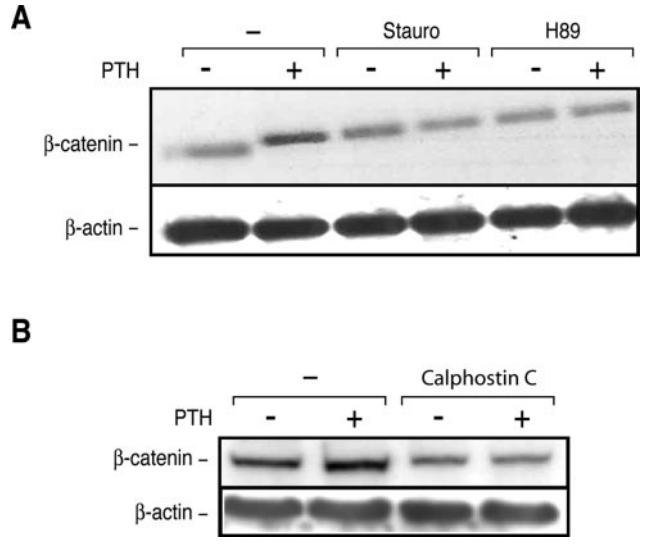

FIG. 3. Effects of PKA and PKC inhibitors on the level of β-catenin induced by PTH in osteoblasts. Confluent MC3T3-E1 cells were cultured in serum-free α-MEM for 12 h, then treated (+) or not (−) with 10^{-8} M PTH-(1–34) for 1 h after having been pretreated (+) or not (−) with (A) 10 nM staurosporine (Stauro) or 10^{-8} M H89 or (B) 500 nM calphostin C for 30 min. Protein extraction of the cells and Western blot analysis were performed as described in *Materials and Methods*.

24 h (Fig. 4C), suggesting that PTH and TGF-β induced β-catenin by a similar mechanism(s) at the later time points. Next, we examined the effects of Smad3 on the levels of β-catenin in these cells. We used stably Smad3-transfected MC3T3-E1 cells, as previously described (10). Smad3-transfected cells had 5-fold higher levels of β-catenin expression (as assessed by Western blot) than empty vector-transfected cells (Fig. 5A). Smad3 overexpression reduced the phosphorylation of β-catenin (serine 45; to 32% of that in empty-vector transfected cells), although Smad3 did not affect the level of β-catenin mRNA (Fig. 5A). These findings indicated that Smad3 induced β-catenin through suppressed degradation of the protein, but not induction of mRNA synthesis. Similar results were obtained in at least three other Smad3-transfected MC3T3-E1 cell clones. We then used a dominant-negative form of Smad3 to examine the role of Smad3 in PTH-induced effects on β-catenin. The truncated Smad3 mutant, Smad3ΔC, lacks the COOH-terminal MH2 region and exerts a dominant-negative effect on endogenous Smad3 activity (14). Smad3 inactivation with Smad3ΔC antagonized PTH-induced β-catenin protein and mRNA levels at 1 h in MC3T3-E1 cells (Fig. 5B). Smad3ΔC antagonism of PTH-induced β-catenin levels was also observed at 24 h (Fig. 5C, *left panel*). The combined findings indicate that PTH stimulates β-catenin expression through Smad3 in osteoblastic

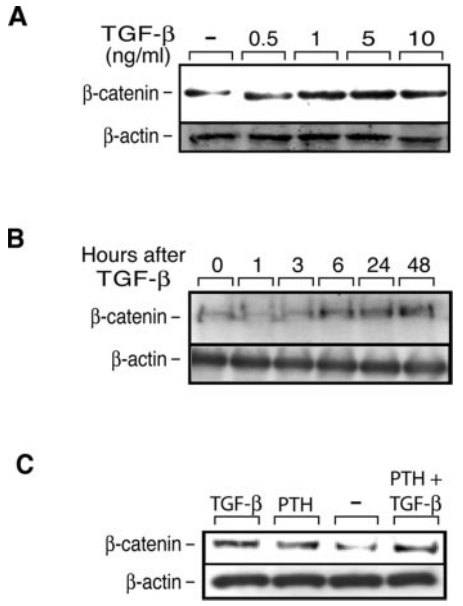

FIG. 4. TGF-β increases the levels of β-catenin in a time- and dose-dependent manner in osteoblasts. Confluent MC3T3-E1 cells were cultured in serum-free α-MEM with TGF-β (A) at the indicated concentrations for 24 h or (B) 5 ng/ml for the indicated times. Protein extraction of the cells and Western blot analysis were performed as described in *Materials and Methods*. C, Confluent MC3T3-E1 cells were cultured without (−) or with 10^{-8} M PTH-(1–34) and/or 5 ng/ml TGF-β for 24 h. Protein extraction of the cells and Western blot analysis were performed as described in *Materials and Methods*.

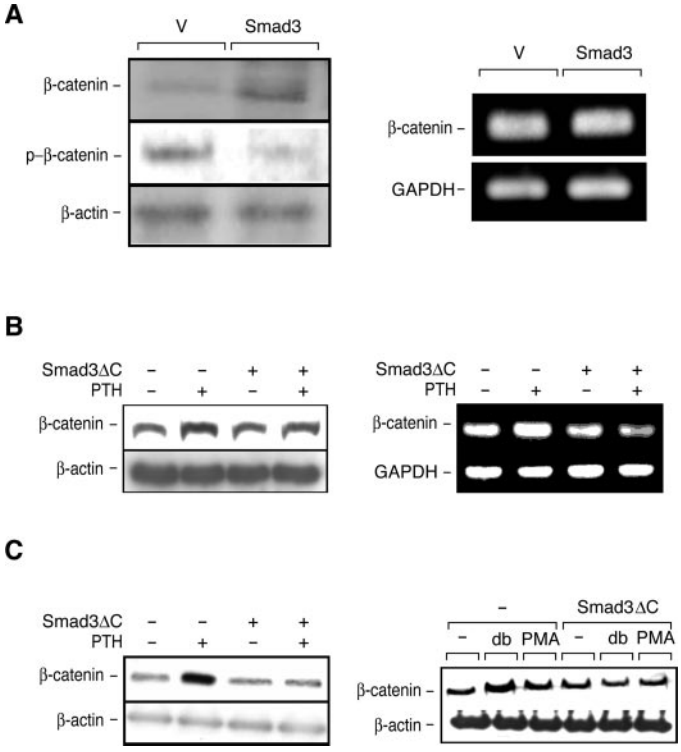

FIG. 5. Smad3 mediates the increases in β-catenin in response to PTH in osteoblasts. A, *Left panel*, Lysates of stably empty vector (V)- or Myc-Smad3 (Smad3)-transfected MC3T3-E1 cells were separated by SDS-PAGE, and Western blotting was carried out with antibodies against β-catenin, phosphorylated β-catenin, and β-actin. *Right panel*, Total RNA was extracted, and semiquantitative RT-PCR analyses of β-catenin and GAPDH were performed as described in *Materials and Methods*. B, Transiently empty vector (−) or Smad3ΔC-transfected MT3T3-E1 cells that had been treated (+) or not (−) with 10^{-8} M PTH-(1–34) for 1 h were analyzed by (*left panel*) Western blot or (*right panel*) RT-PCR analyses as described for A. C, Lysates of transiently empty vector (−) or Smad3ΔC-transfected MC3T3-E1 cells that had been untreated (−) or treated with (*left panel*) 10^{-8} M PTH-(1–34) (+) or (*right panel*) 10^{-4} M db-cAMP (db) or 10^{-6} M PMA for 24 h were separated by SDS-PAGE and Western blotting was carried out with antibodies against β-catenin and β-actin.

cells. Smad3 inactivation with Smad3ΔC also antagonized PKC and PKA activator-induced β-catenin levels (Fig. 5C, *right panel*). The effects of TGF-β on β-catenin as well as on phosphorylated Smad3 were similar in Smad3-overexpressing cells (data not shown). An activation of type II receptors by endogenous or exogenous TGF-β led to activation of the type I receptor. TGF-β type I receptor-like kinase [activin receptor-like kinase 5 (ALK5)] phosphorylated and activated TGF-β receptor-regulated Smad2/3. We used SB431542, which specifically inhibits ALK5 and results in inhibition of endogenous TGF-β action and subsequent phosphorylation of Smad2/3. Moreover, we used cycloheximide as a protein synthesis inhibitor. SB431542 did not affect the PTH-induced β-catenin level at 1 h (Fig. 6A), indicating that PTH induced β-catenin independently of endogenous TGF-β and phosphorylation of Smad3 at the early time points. In contrast, SB431542 as well as cycloheximide antagonized PTH-induced β-catenin levels at 24 h (Fig. 6B), indicating that PTH induced β-catenin through protein synthesis, induction of endogenous TGF-β, and subsequent phosphorylation of Smad3 at the later time points.

Effects of PTH on transcriptional activity induced by β-catenin in mouse osteoblastic cells

We next investigated whether PTH affects the transcriptional activity stimulated by the Wnt-β-catenin pathway in MC3T3-E1 cells. We used the pGL3-OT luciferase reporter plasmid that has Tcf/Lef binding elements in the promoter and is commonly used to examine β-catenin-induced transcriptional activity (15). In the absence of activated β-catenin, PTH did not induce transcriptional activity (data not shown). Therefore, we examined the effects of PTH on transcriptional activity in cells in which the activated β-catenin was coexpressed. PTH enhanced the luciferase activity of the transfected promoter-reporter construct induced by activated β-catenin in MC3T3-E1 cells (Fig. 7). Cotransfection with the dominant-negative Smad3ΔC antagonized PTH-induced transcriptional activity (Fig. 7). These findings indicate that PTH enhances the transcriptional activity induced by β-catenin through Smad3.

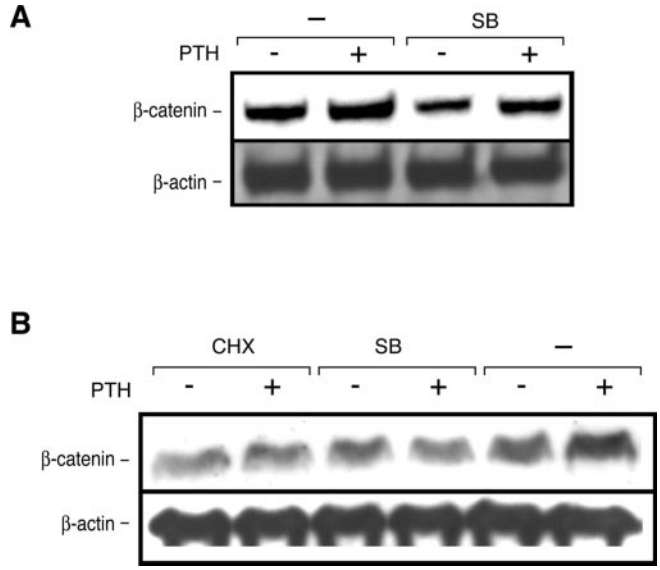

FIG. 6. Effects of ALK5 and protein synthesis inhibitors on the levels of β-catenin induced by PTH in osteoblasts. Confluent MC3T3-E1 cells were cultured in serum-free α-MEM for 12 h, then treated (+) or not (−) with 10^{-8} M PTH-(1–34) for 1 h (A) or 24 h (B) after having been pretreated (+) or not (−) with 1 μM SB431542 (SB) or 10 μM cycloheximide (CHX) for 30 min and 6 h, respectively. Protein extraction of the cells and Western blot analysis were performed as described in *Materials and Methods*.

Role of Wnt-β-catenin signaling in the suppression of apoptosis induced by PTH in osteoblastic cells

We and others previously reported that PTH exerts antiapoptotic actions in osteoblasts (14, 19, 20). Lithium inhibits glycogen synthase kinase-3β activity and leads to a significant increase in endogenous β-catenin signaling activity (21, 22). Therefore, we next used $LiCl_2$ to examine the role of Wnt-β-catenin signaling in osteoblasts with respect to apoptosis. Trypan blue staining was used as a general method to distinguish viable from nonviable cells, whereas the TUNEL method was used to specifically detect apoptosis. Dexamethasone and etoposide increased the number of dead cells in MC3T3-E1 cells (Fig. 8A). Treatment with PTH-(1–34) as well as $LiCl_2$ antagonized dexamethasone- and etoposide-induced cell death in both types of experiment (Fig. 8). The combined treatment with either PTH-(1–34) or $LiCl_2$ rescued cell death to the same extent as that achieved with each alone (Fig. 8). These results suggest that both PTH and Wnt-β-catenin act in part through a common pathway to rescue osteoblasts from apoptosis. Cotransfection with Smad3ΔC antagonized the PTH-induced antiapoptotic effects (Fig. 9). This is compatible with data obtained in UMR106 osteoblastic cells that we had previously reported (14). Smad3 inactivation with Smad3ΔC did not affect the inhibition of dexamethasone-induced apoptosis by $LiCl_2$ (Fig. 9). Moreover, activated β-catenin transfection significantly rescued dexamethasone-induced apoptosis.

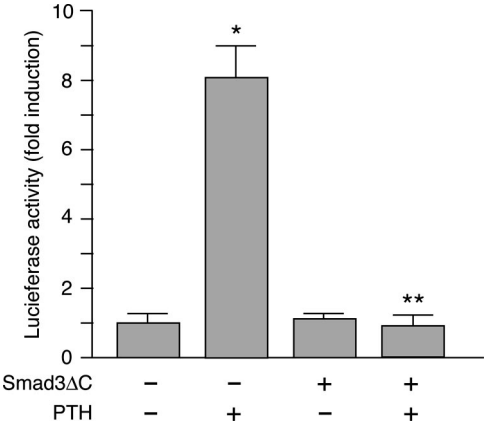

FIG. 7. PTH enhances the transcriptional activity induced by β-catenin. MC3T3-E1 cells were transfected with the β-catenin-responsive luciferase reporter plasmid (pGL3-OT), the activated β-catenin cDNA vector, and the β-galactosidase-expressing pCH110 plasmid without (−) or with (+) the Smad3ΔC vector. Twenty-four hours later, cells were treated without (−) or with (+) 10^{-8} M PTH-(1–34) for 24 h. Then the cells were harvested, and relative luciferase activity was measured. Values are the mean ± SEM. *, $P < 0.01$ compared with the Smad3ΔC (−), PTH (−) group; **, $P < 0.01$ compared with the Smad3ΔC (−), PTH (+) group.

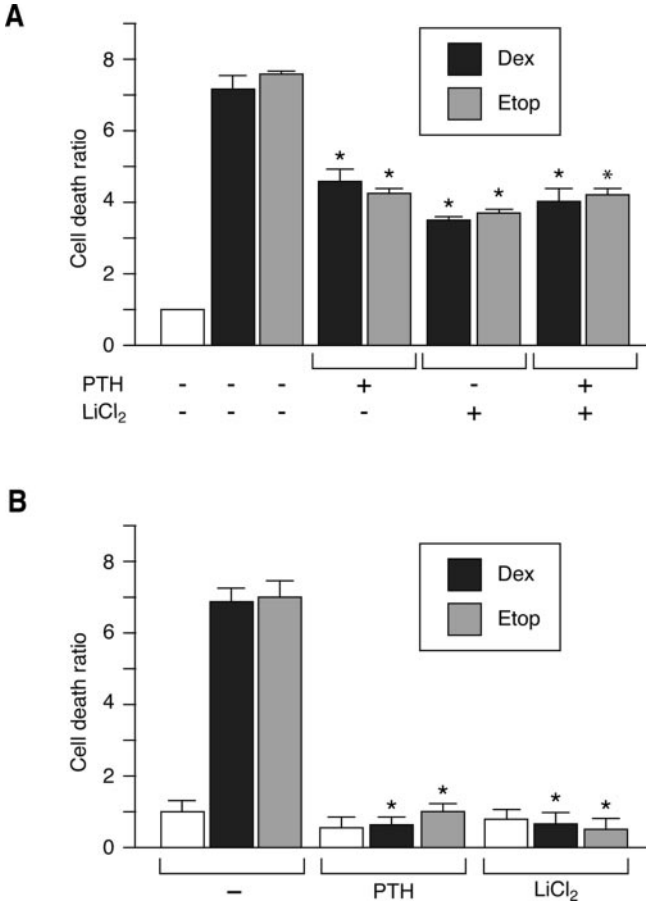

FIG. 8. PTH and $LiCl_2$ reverse dexamethasone- and etoposide-mediated cell death in osteoblasts. MC3T3-E1 cells were treated with 10^{-7} M dexamethasone (Dex) or 5×10^{-5} M etoposide (Etop) for 6 h without (−) or with pretreatment with 10^{-8} M PTH-(1–34) and/or 25 mM $LiCl_2$ for 1 h in serum-free α-MEM. A, The relative number of nonviable cells was determined by trypan blue staining; B, the relative number of apoptotic cells was determined by TUNEL assay, as described in *Materials and Methods*. Values are the mean ± SEM of the ratio of A, trypan blue positive/negative cell numbers or B, TUNEL positive/negative cell numbers compared with Dex- or Etop-untreated cells (−). *, $P < 0.01$, compared with the corresponding PTH and/ or $LiCl_2$-untreated group.

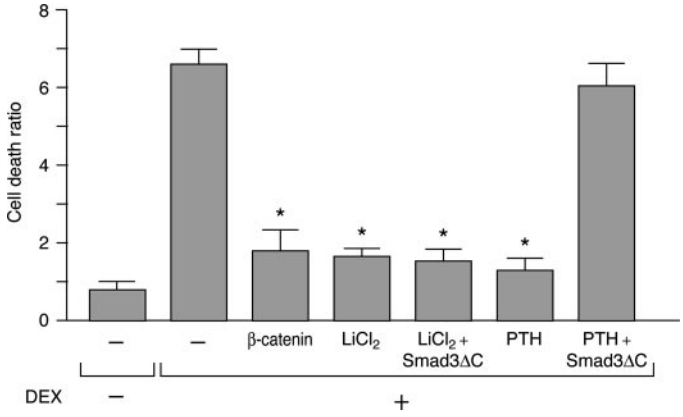

FIG. 9. Activated β-catenin reverses dexamethasone (Dex)-mediated cell apoptosis independently of Smad3 in osteoblasts. MC3T3-E1 cells with or without transient activated β-catenin or Smad3ΔC transfection were treated without (−) or with 10^{-7} M Dex for 6 h without or with pretreatment with 10^{-8} M PTH-(1–34) and/or 25 mM $LiCl_2$ for 1 h in serum-free α-MEM. The relative number of apoptotic cells was determined by TUNEL assay as described in *Materials and Methods*. Values are the mean ± SEM ratio of TUNEL positive/negative cell numbers compared with Dex-untreated cells. *, $P < 0.01$ compared with Dex-only-treated cells.

Discussion

The bone anabolic action of PTH *in vivo* involves in part the up-regulation of osteoblast growth factors, such as IGF-I and TGF-β, which act via signaling pathways that lead to altered gene transcription (23–25). Also, PTH increases Runx2 expression, the key osteoblast-specific transcriptional regulator (26), and a physical interaction between Runx2 and AP-1 is required for PTH-stimulated transcriptional activity of the collagenase-3 promoter in osteoblasts (27). Overall, there is abundant evidence that transcriptional regulation is critical for the bone anabolic action of PTH.

The present study demonstrated that PTH increases the level of β-catenin in mouse osteoblastic cells. Moreover, we showed that PTH enhances the transcriptional activity induced by activated β-catenin in osteoblastic cells. Our findings and those of others (28, 29) suggest that PTH induces the canonical Wnt-β-catenin pathway in osteoblasts. Mice with targeted disruption of LRP5 develop a low bone mass phenotype, which is secondary to decreased osteoblast proliferation and function (30). Moreover, activated β-catenin induces osteoblast differentiation of mouse pluripotent C3H10T1/2 cells (22), and the effects of bone morphogenetic protein-2 on extracellular matrix mineralization by osteoblasts are mediated by a Wnt autocrine/paracrine loop in mesenchymal C3H10T1/2, C2C12, ST2 cells, and MC3T3-E1 cells (31). Increases in β-catenin levels lead to the nuclear translocation of Lef/Tcf transcription factors, resulting in transcriptional activation of Wnt target genes (3). Therefore, the work of others and the present study provide the link between PTH induction of the Wnt-β-catenin pathway and bone formation in osteoblasts.

The role of PKA and PKC signaling pathways in bone formation is controversial. Some researchers reported that PTH exerts antiapoptotic actions in osteoblasts through PKA signaling (19). Others have reported that intermittent treatment with PTH stimulates bone anabolism through both PKA and PKC pathways in osteoblasts (20). However, it has been reported that PKC activity inhibits osteoblast differentiation (32). In our study, both PKA and PKC activators as well as PTH-(3–34) increased the level of β-catenin, and both PKA and PKC inhibitors antagonized the increase in β-catenin stimulated by PTH in MC3T3-E1 cells. Recently, a study using the UMR106 osteoblastic cell line suggested an effect of PTH on the canonical Wnt signaling pathway via the cAMP-PKA pathway (33). However, involvement of the PKC pathway was not demonstrated. Our findings indicate that PTH increases the level of β-catenin in osteoblasts through both PKA and PKC signaling pathways.

TGF-β increases the level of β-catenin in human mesenchymal progenitor cells (34). Moreover, Smad3 interacts and synergizes with Lef1 to activate gene expression signaled by TGF-β (35). However, whether TGF-β or its signaling molecule, Smad3, would affect Wnt-β-catenin signaling in os-

teoblasts was not known. Our recent study revealed that PTH promotes the expression of Smad3 within 1 h in osteoblastic cells (14). Moreover, our present study demonstrated that Smad3 induces the expression of β-catenin, and inactivation of Smad3 antagonizes PTH-induced β-catenin expression in MC3T3-E1 cells. Taken together, these findings indicate that PTH increases the expression of β-catenin through Smad3 in osteoblasts.

Smad3 is a critical component of the TGF-β signaling pathway. Previous studies indicated that PTH stimulates TGF-β expression in osteoblasts (36), and we previously reported that PTH induces the expression of TGF-β after 6 h in MC3T3-E1 cells (14). In contrast, PTH stimulates Smad3 expression as early as 1 h, an effect that is independent of *de novo* protein synthesis (14). Moreover, the present study revealed that PTH elevates the level of β-catenin within 1 h, with additional elevation continuing after 6 h. In addition, the induction of β-catenin by TGF-β starts after 6 h in MC3T3-E1 cells. These findings indicated that at least the early induction of β-catenin levels by PTH is not through TGF-β. The Wnt-β-catenin pathway might play a regulatory role downstream of the PTH-Smad3 axis in osteoblasts. Alternatively, PTH might induce Smad3 by enhancing the action of endogenous TGF-β in the bone microenvironment. SB431542 is useful in inhibiting the action of endogenous TGF-β in osteoblastic cells (37). The present data suggest that PTH causes an early induction of β-catenin levels independently of endogenous TGF-β action and subsequent phosphorylation of Smad3. Moreover, we have found in preliminary work that transfection of a Smad3 dominant-negative mutant in which the COOH-terminal SSXS motif (that is phosphorylated and activates Smad3 in response to activation of ALK5/TGF-β type I receptors) had been mutated to AAXA antagonized the later phase induction of β-catenin by PTH, but not the early phase (data not shown). In contrast, PTH induces a later enhancement of β-catenin, presumably through the induction of endogenous TGF-β. Although TGF-β induced β-catenin levels from 6 h and an early induction of β-catenin by PTH started within 1 h, it remains unknown why TGF-β requires more time than PTH to increase β-catenin. The PTH-Smad3 axis might induce β-catenin through a Smad-dependent pathway other than the classical TGF-β-Smad signaling pathway. However, the detailed mechanism by which Smad3 induces β-catenin is not known. Additional study is necessary to clarify these issues.

Apoptosis plays a critical role during embryonic limb development, skeletal maturation, bone turnover, fracture healing, and bone degeneration. The balance of osteoblast proliferation, differentiation, and apoptosis determines the size of the osteoblast population at any given time (38). In the present study, PTH as well as $LiCl_2$, which mimics the effects of Wnt-β-catenin signaling, exhibited antiapoptotic effects on osteoblasts. In human osteoblastic cell lines, the proteolytic cleavage of β-catenin is associated with the activation of caspase-3 and induces osteoblast apoptosis, suggesting that activation of β-catenin signaling promotes osteoblast survival (39). Furthermore, a report that was recently published (while our manuscript was under review) showed that Wnt-β-catenin signaling prevents apoptosis of both uncommitted osteoblast progenitors and differentiated osteoblasts, including MC3T3-E1 cells (40). Moreover, our previous study indicated that PTH exerts antiapoptotic actions on osteoblasts through Smad3, a crucial mediator of TGF-β signaling (14). In that study, PTH increased the level of Smad3 through both PKA and PKC pathways, which also supports the idea that both signaling pathways are involved, as indicated in the present study. Based on these lines of evidence and the present data, β-catenin is likely to be important for the antiapoptotic effects of PTH in osteoblasts. It is possible that the cross-talk among the actions of PTH, Smad3, and Wnt is coordinated to exert antiapoptotic effects in osteoblasts. In the present study, Smad3 inactivation by a dominant-negative Smad3 antagonized the enhancement of expression and transcriptional activity of β-catenin by PTH. Moreover, our previous study showed that Smad3 inactivation antagonizes the inhibition of dexamethasone- and etoposide-induced apoptosis brought about by PTH in osteoblasts, including MC3T3-E1 cells. Overall, the findings provide evidence that PTH increases the level of β-catenin through Smad3, resulting in the activation of canonical Wnt-β-catenin signaling. Moreover, PTH induction of the Smad3-Wnt-β-catenin pathway appears to lead to the inhibition of apoptosis; however, additional studies of specific direct inhibition of β-catenin action will be needed to confirm this.

A recent study revealed that PTH increased the level of β-catenin within 1 h in rat osteoblastic UMR-106 cells (33). We confirmed this finding in UMR-106 cells. Furthermore, we observed that inactivation of Smad3 by Smad3ΔC antagonized the PTH-induced increases in β-catenin levels and transcriptional activity in UMR-106 cells (preliminary data not shown), similar to what we report in this study in MC3T3-E1 osteoblastic cells.

Our data indicate that PTH augments β-catenin-induced transcriptional activity, although β-catenin inhibition of the apoptotic effect is not necessarily always PTH dependent. The preventative effect of transfected β-catenin on apoptosis in the absence of PTH is probably due to the overexpression of β-catenin. This phenomenon is common for overexpression-type experiments. Indeed, this experimental paradigm is often used to provide evidence of linkage of one event to another, as in our study.

In conclusion, our data show that PTH increases the level of β-catenin expression in mouse osteoblastic cells via both PKA- and PKC-signaling pathways. Moreover, Smad3 is directly involved in this enhancement of β-catenin levels. PTH or activation of the Wnt-β-catenin pathway reverses osteoblast apoptosis. PTH may well exert antiapoptotic actions by stimulating the activity of Wnt-β-catenin signaling in osteoblasts; additional studies will help to clarify this issue.

Acknowledgments

We thank Drs. J. J. Lebrun, Y. Chen, R. Farookhi, and B. Vogelstein for providing plasmids, and acknowledge Mrs. Y. Higashimaki and Miss K. Takeuchi for excellent technical support.

Received December 20, 2005. Accepted February 6, 2006.

Address all correspondence and requests for reprints to: Dr. Hiroshi Kaji, Division of Endocrinology/Metabolism, Neurology, and Hematology/Oncology, Department of Clinical Molecular Medicine, Kobe University Graduate School of Medicine, 7-5-1 Kusunoki-cho, Chuo-ku, Kobe 650-0017, Japan. E-mail: hiroshik@med.kobe-u.ac.jp.

This work was supported by the Takeda Science Foundation (to H.K.); a grant-in-aid from the Ministry of Science, Education, and Culture of Japan [17590961 (to H.K.) and 16590906 (to T.S.)]; a grant-in-aid from the Hormone Receptor Abnormality Research Committee Ministry of Health and Welfare of Japan (to T.S.); and Canadian Institutes of Health Research Grant MOP-9315 (to G.N.H.).

All listed authors have nothing to declare.

References

1. **Dempster DW, Cosman F, Parisien M, Shen V, Lindsay R** 1993 Anabolic actions of parathyroid hormone on bone. Endocr Rev 14:690–709
2. **Swarthout JT, D'Alonzo RC, Selvamurugan N, Partridge NC** 2002 Parathyroid hormone-dependent signaling pathways regulating genes in bone cells. Gene 282:1–17
3. **Moon RT, Bowerman B, Boutros M, Perrimon N** 2002 The promise and perils of Wnt signaling through β-catenin. Science 296:1644–1646
4. **Behrens J, von Kries JP, Kuhl M, Bruhn L, Wedlich D, Grosschedl R, Birchmeier W** 1996 Functional interaction of β-catenin with the transcription factor LEF-1. Nature 382:638–642
5. **Gong Y, Slee RB, Fukai N, Rawadi G, Roman-Roman S, Reginato AM, Wang H, Cundy T, Glorieux FH, Lev D, Zacharin M, Oexle K, Marcelino J, Suwairi W, Heeger S, Sabatakos G, Apte S, Adkins WN, Allgrove J, Arslan-Kirchner M, Batch JA, Beighton P, Black GC, Boles RG, Boon LM, Borrone C, Brunner HG, Carle GF, Dallapiccola B, De Paepe A, Floege B, Halfhide ML, Hall B, Hennekam RC, Hirose T, Jans A, Juppner H, Kim CA, Keppler-Noreuil K, Kohlschuetter A, LaCombe D, Lambert M, Lemyre E, Letteboer T, Peltonen L, Ramesar RS, Romanengo M, Somer H, Steichen-Gersdorf E, Steinmann B, Sullivan B, Superti-Furga A, Swoboda W, Van den Boogaard MJ, Van Hul W, Vikkula M, Votruba M, Zabel B, Garcia T, Baron R, Olsen BR, Warman ML** 2001 LDL receptor-related protein 5 (LRP5) affects bone accrual and eye development. Cell 107:513–523
6. **Boyden LM, Mao J, Belsky J, Mitzner L, Farhi A, Mitnick MA, Wu D, Insogna K, Lifton RP** 2002 High bone density due to a mutation in LDL-receptor-related protein 5. N Engl J Med 346:1513–1521
7. **Kolpakova E, Olsen BR** 2005 Wnt/β-catenin: a canonical tale of cell-fate choice in the vertebrate skeleton. Dev Cell 8:626–627
8. **Holmen SL, Zylstra CR, Mukherjee A, Sigler RE, Faugere MC, Bouxsein ML, Deng L, Clemens TL, Williams BO** 2005 Essential role of β-catenin in postnatal bone acquisition. J Biol Chem 280:21162–21168
9. **Hens JR, Wilson KM, Dann P, Chen X, Horowitz MC, Wysolmerski JJ** 2005 TOPGAL mice show that the canonical Wnt signaling pathway is active during bone development and growth and is activated by mechanical loading in vitro. J Bone Miner Res 20:1103–1113
10. **Sowa H, Kaji H, Yamaguchi T, Sugimoto T, Chihara K** 2002 Smad3 promotes alkaline phosphatase activity and mineralization of osteoblastic MC3T3-E1 cells. J Bone Miner Res 17:1190–1199
11. **Sowa H, Kaji H, Yamaguchi T, Sugimoto T, Chihara K** 2002 Activations of ERK1/2 and JNK by transforming growth factor β negatively regulate Smad3-induced alkaline phosphatase activity and mineralization in mouse osteoblastic cells. J Biol Chem 277:36024–36031
12. **Borton AJ, Frederick JP, Datto MB, Wang XF, Weinstein RS** 2001 The loss of Smad3 results in a lower rate of bone formation and osteopenia through dysregulation of osteoblast differentiation and apoptosis. J Bone Miner Res 16:1754–1764
13. **Lebrun JJ, Takabe K, Chen Y, Vale W** 1999 Roles of pathway-specific and inhibitory Smads in activin receptor signaling. Mol Endocrinol 13:15–23
14. **Shih IM, Yu J, He TC, Vogelstein B, Kinzler KW** 2000 The β-catenin binding domain of adenomatous polyposis coli is sufficient for tumor suppression. Cancer Res 60:1671–1676
15. **Morin PJ, Sparks AB, Korinek V, Barker N, Clevers H, Vogelstein B, Kinzler KW** 1997 Activation of β-catenin-Tcf signaling in colon cancer by mutations in β-catenin or APC. Science 275:1787–1790
16. **Kaji H, Canaff L, Lebrun JJ, Goltzman D, Hendy GN** 2001 Inactivation of menin, a Smad3-interacting protein, blocks transforming growth factor-β signaling. Proc Natl Acad Sci USA 98:3837–3842
17. **Sowa H, Kaji H, Iu MF, Tsukamoto T, Sugimoto T, Chihara K** 2003 Parathyroid hormone-Smad3 axis exerts anti-apoptotic action and augments anabolic action of transforming growth factor β in osteoblasts. J Biol Chem 278:52240–52252
18. **Yost C, Torres M, Miller JR, Huang E, Kimelman D, Moon RT** 1996 The axis-inducing activity, stability, and subcellular distribution of β-catenin is regulated in *Xenopus* embryos by glycogen synthase kinase 3. Genes Dev 10:1443–1454
19. **Jilka RL, Weinstein RS, Bellido T, Roberson P, Parfitt AM, Manolagas SC** 1999 Increased bone formation by prevention of osteoblast apoptosis with parathyroid hormone. J Clin Invest 104:439–446
20. **Ishizuya T, Yokose S, Hori M, Noda T, Suda T, Yoshiki S, Yamaguchi A** 1997 Parathyroid hormone exerts disparate effects on osteoblast differentiation depending on exposure time in rat osteoblastic cells. J Clin Invest 99:2961–2970
21. **Stambolic V, Ruel L, Woodgett JR** 1996 Lithium inhibits glycogen synthase kinase-3 activity and mimics wingless signalling in intact cells. Curr Biol 6:1664–1668
22. **Bain G, Muller T, Wang X, Papkoff J** 2003 Activated β-catenin induces osteoblast differentiation of C3H10T1/2 cells and participates in BMP2 mediated signal transduction. Biochem Biophys Res Commun 301:84–91
23. **Pfeilschifter J, Laukhuf F, Muller-Beckmann B, Blum WF, Pfister T, Ziegler R** 1995 Parathyroid hormone increases the concentration of insulin-like growth factor-I and transforming growth factor β1 in rat bone. J Clin Invest 96:767–774
24. **Linkhart TA, Mohan S** 1989 Parathyroid hormone stimulates release of insulin-like growth factor-I (IGF-I) and IGF-II from neonatal mouse calvaria in organ culture. Endocrinology 125:1484–1491
25. **Rosen CJ, Bilezikian JP** 2001 Clinical review 123: Anabolic therapy for osteoporosis. J Clin Endocrinol Metab 86:957–964
26. **Selvamurugan N, Pulumati MR, Tyson DR, Partridge NC** 2000 Parathyroid hormone regulation of the rat collagenase-3 promoter by protein kinase A-dependent transactivation of core binding factor α1. J Biol Chem 275:5037–5042
27. **D'Alonzo RC, Kowalski AJ, Denhardt DT, Nickols GA, Partridge NC** 2002 Regulation of collagenase-3 and osteocalcin gene expression by collagen and osteopontin in differentiating MC3T3-E1 cells. J Biol Chem 277:24788–24798
28. **Bodine PVN, Kharode YP, Seestaller-Wehr L, Green P, Milligan C, Bex FJ** 2004 The bone anabolic effects of parathyroid hormone (PTH) are blunted by deletion of the Wnt antagonist secreted frizzled-related protein (sFRP)-1. J Bone Miner Res 19(Suppl 1):S17
29. **Leman ES, Bencsik M, Nguyen P, Marvi U, Nissenson RA** 2004 Synergistic actions of parathyroid hormone and β-catenin in the canonical Wnt signaling pathway in osteoblastic cells. J Bone Miner Res 19(Suppl 1):S105
30. **Kato M, Patel MS, Levasseur R, Lobov I, Chang BH, Glass 2nd DA, Hartmann C, Li L, Hwang TH, Brayton CF, Lang RA, Karsenty G, Chan L** 2002 Cbfa1-independent decrease in osteoblast proliferation, osteopenia, and persistent embryonic eye vascularization in mice deficient in Lrp5, a Wnt coreceptor. J Cell Biol 157:303–314
31. **Rawadi G, Vayssiere B, Dunn F, Baron R, Roman-Roman S** 2003 BMP-2 controls alkaline phosphatase expression and osteoblast mineralization by a Wnt autocrine loop. J Bone Miner Res 18:1842–1853
32. **Ogata N, Roth SI, Kawaguchi H, Segre GV** 2002 Activation of PKC by Gαq results in osteopenia by blocking osteoblast differentiation. J Bone Miner Res 17(Suppl 1):S138
33. **Kulkarni NH, Halladay DL, Miles RR, Gilbert LM, Frolik CA, Galvin RJ, Martin TJ, Gillespie MT, Onyia JE** 2005 Effects of parathyroid hormone on Wnt signaling pathway in bone. J Cell Biochem 95:1178–1190
34. **Tuli R, Tuli S, Nandi S, Huang X, Manner PA, Hozack WJ, Danielson KG, Hall DJ, Tuan RS** 2003 Transforming growth factor-β-mediated chondrogenesis of human mesenchymal progenitor cells involves N-cadherin and mitogen-activated protein kinase and Wnt signaling cross-talk. J Biol Chem 278:41227–41236
35. **Labbe E, Letamendia A, Attisano L** 2000 Association of Smads with lymphoid enhancer binding factor 1/T cell-specific factor mediates cooperative signaling by the transforming growth factor-β and wnt pathways. Proc Natl Acad Sci USA 97:8358–8363
36. **Wu Y, Kumar R** 2000 Parathyroid hormone regulates transforming growth factor β1 and β2 synthesis in osteoblasts via divergent signaling pathways. J Bone Miner Res 15:879–884
37. **Maeda S, Hayashi M, Komiya S, Imamura T, Miyazono K** 2004 Endogenous TGF-β signaling suppresses maturation of osteoblastic mesenchymal cells. EMBO J 23:552–563
38. **Hock JM, Krishnan V, Onyia JE, Bidwell JP, Milas J, Stanislaus D** 2001 Osteoblast apoptosis and bone turnover. J Bone Miner Res 16:975–984
39. **Hunter I, McGregor D, Robins SP** 2001 Caspase-dependent cleavage of cadherins and catenins during osteoblast apoptosis. J Bone Miner Res 16:466–477
40. **Almeida M, Han L, Bellido T, Manolagas SC, Kousteni S** 2005 Wnt proteins prevent apoptosis of both uncommitted osteoblast progenitors and differentiated osteoblasts by β-catenin-dependent and -independent signaling cascades involving Src/ERK and phosphatidylinositol 3-kinase/AKT. J Biol Chem 280:41342–41351

Endocrinology **is published monthly by The Endocrine Society (http://www.endo-society.org), the foremost professional society serving the endocrine community.**